

Assessment of Subchannel Temperature Distributions in the WARD 61-Rod Heat Transfer Experiment Using the SLTHEN Code

Sun Rock Choi*, Jonggan Hong, Jaehyuk Eoh

Korea Atomic Energy Research Institute, 111, Daedeok-daero 989Beon-gil, Yuseong-gu, Daejeon 34057, Republic of Korea

*Corresponding author: choisr@kaeri.re.kr

1. Introduction

The core thermal-hydraulic design is used to ensure an appropriate margin for fuel safety limits. The typical fuel safety limit employed in a pressurized water reactor (PWR) design is the departure from the nucleate boiling ratio (DNBR) on fuel cladding surface. On the other hand, in a sodium-cooled fast reactor (SFR), DNBR is not a concern because of the high thermal conductivity (hundreds of times larger than water) and high boiling temperature (around 900°C at the normal operating condition) of sodium coolant, and nuclear fuel damage commonly arises from a creep induced failure. The creep limit is evaluated based on the maximum cladding temperature considering the uncertainties of the design parameters. An accurate temperature calculation in each subassembly is highly important to assure a safe and reliable operation of reactor systems.

The core thermal-hydraulic design in the KAERI is performed using the SLTHEN (Steady-State LMR Thermal-Hydraulic Analysis Code Based on ENERGY Model) code, which calculates the temperature distribution based on the ENERGY model[1]. In this work, the SLTHEN code is validated using subchannel temperature distributions in the WARD 61-rods heat transfer experiments[2].

2. SLTHEN code

The subchannel analysis is generally employed for core thermal-hydraulic design. Assuming that the axial flow rate is dominant over the radial flow change in a rod bundle, the bulk average value in axial control volume of each subchannel is calculated by solving the governing equations. The simplicity of subchannel analysis enhances the efficiency in both computer storage and run time but needs predefined parameters that appropriately characterize the thermal-hydraulic conditions averaged by each subchannel.

The SLTHEN code employs two-region approximations to describe these subchannel flow characteristics as shown in Fig. 1. The central region represents the interior subchannels. The wall region includes the edge and corner subchannels. In the central region, the axial velocity is uniform and the lateral flow oscillates around each rod as it progresses along the axial direction. In the outer region near the wall, the circumferential flow pattern is developed along the hexagonal ducts. This difference in the outer and inner

regions of the assembly suggests that the entire subassembly flow feature can be divided into two regions. As shown in Fig. 1, region I is the inner region where the wire wrap mixing effect can be modeled by effective eddy diffusivity. Region II is the outer region, which can be additionally modeled by an average circumferential swirl flow due to the unidirectional wire wrap in this flow region. The pre-calculated flow parameters enable the momentum equations to be decoupled from the energy equations.

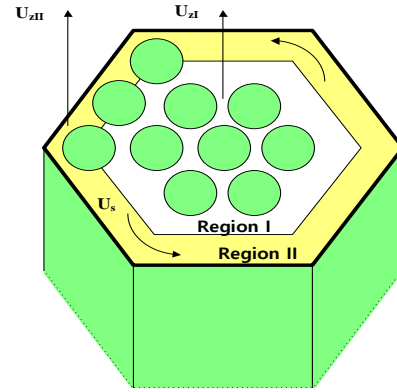


Fig. 1. Two region model in the SLTHEN code

To illustrate the cross-flow patterns between subchannels without momentum equations, the ENERGY model uses effective eddy diffusivity (ϵ) in the central region and circumferential velocity in the outer region due to wire-wraps. From a flow split model between the central and outer regions, two axial velocities are determined. The resulting energy transport equations for the two regions are then calculated by

$$\rho C_p U_{zI} \frac{\partial T}{\partial z} = (\rho C_p \epsilon_I + \zeta k) \left(\frac{\partial^2 T}{\partial x^2} + \frac{\partial^2 T}{\partial y^2} \right) + Q \quad (1)$$

$$\begin{aligned} \rho C_p U_s \frac{\partial T}{\partial s} + \rho C_p U_{zII} \frac{\partial T}{\partial z} \\ = (\rho C_p \epsilon_n + \zeta k) \frac{\partial^2 T}{\partial n^2} + (\rho C_p \epsilon_s + \zeta k) \frac{\partial^2 T}{\partial s^2} + Q \end{aligned} \quad (2)$$

where the left and right terms represent convective heat transfer and conduction by the enhanced eddy diffusivity, respectively. Q , k and ζ are the volumetric heat source, coolant thermal conductivity and conductivity enhancement ratio from the geometrical factor.

3. WARD 61-rods experiment

The Westinghouse Advanced Reactors Division (WARD) conducted the heat transfer test in wire wrapped rod bundles using electrically heated fuel rod simulators in flowing sodium[2]. The test section is designed to be similar to actual SFR assembly as shown in Fig. 2. The radial and axial power distributions are simulated for various positions in a reactor by the fuel rod simulators. The test assembly consists of 61-rod bundle of 1.318 cm diameter. Each rod is wrapped with a spacer wire of 0.094 cm diameter. The WARD 61-rod test was performed to verify the sodium cooling properties of the blanket assembly. Therefore, the pitch to diameter ratio of the simulated fuel rod is very small to be 1.082. The fuel rod simulators supply heat from 24.1cm to 140cm in the axial direction.

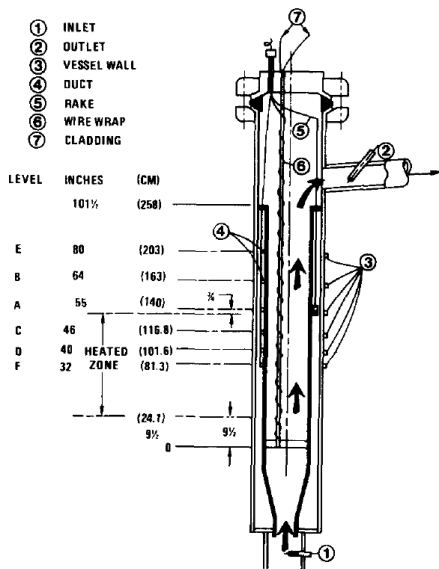


Fig. 2. Schematic diagram of the WARD 61-rod assembly[2]

The thermocouples were located at selected elevations as shown in Fig. 2. At each elevation, the thermocouples provide radial temperature distributions to characterize heat transfer. The heat transfer within the test assembly reveals the single-phase characteristic and thermo-physical property variation is generally very small. Therefore, the validation tests used a smaller heating power than that of actual reactors, and simply accessed a relative temperature distribution to the inlet/outlet temperature difference.

$$\Delta \bar{T} = \frac{T_{sub} - T_{in}}{T_{out} - T_{in}} \quad (3)$$

4. Results

Figures 3-5 provide the code predictions and the experimental data with different power peaking. The calculation utilizes three flow distribution models such as Novendstern, Chiu-Rohsenow-Todreas, and Cheng-

Todreas correlations. The code calculations show good agreement with the experimental data. However, the three friction correlations represent flow-split differences between the inner and outer subchannels and the corresponding different maximum temperature in the subassembly central regions. The power peaking distorts the radial temperature distribution and increase the maximum temperature within a subassembly.

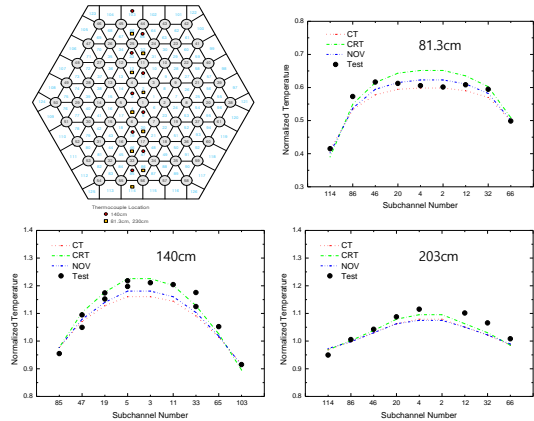


Fig. 3. Thermocouple and temperature distributions with uniform heating

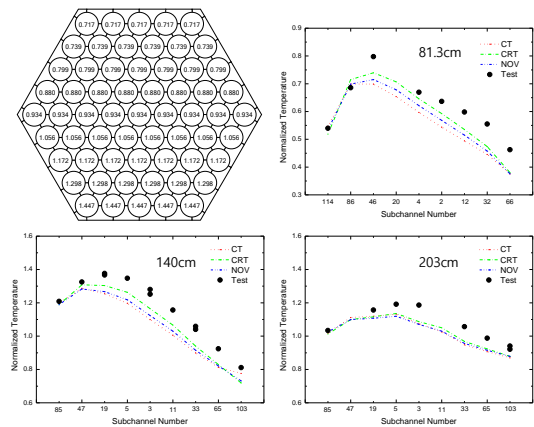


Fig. 4. Rod power and temperature distributions with 2.0/1 power peaking

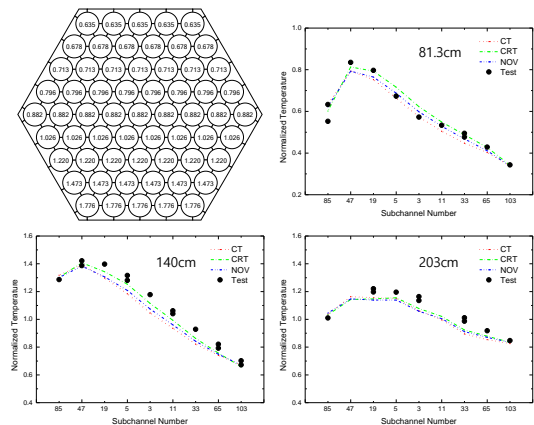


Fig. 5. Rod power and temperature distributions with 2.8/1 power peaking

grant funded by the Korean government (MSIT) [grant numbers 2021M2E2A2081061, CAP-20-03-KAERI].

REFERENCES

- [1] W. S. Yang, An LMR Core Thermal-Hydraulics Code Based on the ENERGY Model, Journal of the Korean Nuclear Society, Vol. 29, pp. 406-416, 1997.
- [2] F. C. Engel, et al., "Characterization of Heat Transfer and Temperature Distributions in an Electrically Heated Model of an LMFBR Blanket Assembly," Nuclear Engineering and Design, Vol. 62, pp. 335-347, 1980.

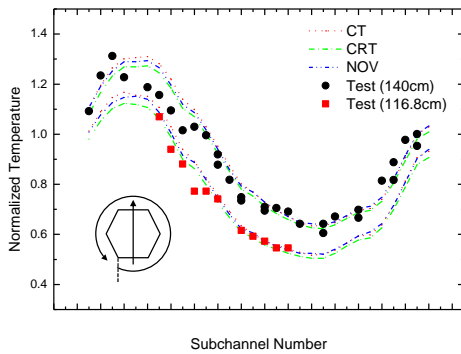


Fig. 6. Temperature distribution in edge subchannels with 2.8/1 power peaking

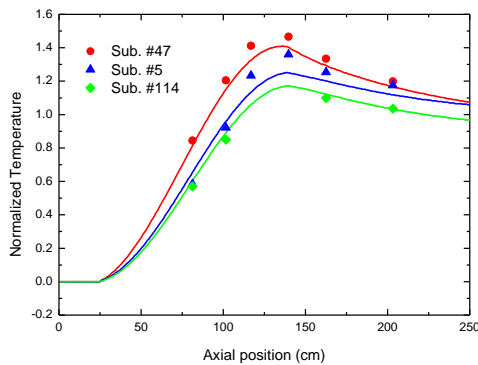


Fig. 7. Axial temperature distribution with 2.8/1 power peaking

Figure 6 displays the temperature distributions with 2.8/1 power peaking in edge subchannels. The results reveal the power peaking effect on the temperature rise along duct walls. Figure 7 shows an axial temperature rise for the same condition. Since the fuel rod simulators supply heat from 24.1cm to 140cm in the axial direction, the temperature increases as thermal energy accumulates along the heater region. The axial temperature reduction in the central region also indicates a radial mixing effect through which temperature distribution becomes flat from the end of the heated zone.

5. Conclusions

The SLTHEN code validation for the core thermal-hydraulic design has been performed using subchannel temperature distributions in the WARD 61-rods heat transfer experiments. The results indicate that the SLTHEN code appropriately predicts the temperature distributions of the WARD 61-rod experimental values. Major discrepancy is observed at the maximum temperature in the central region.

ACKNOWLEDGEMENT

This work was supported by the National Research Foundation of Korea, Republic of Korea (NRF) grant and National Research Council of Science & Technology (NST)